Molecular characterization of an acidic phospholipase A 2 from Bothrops pirajai snake venom: Synthetic C-terminal peptide identifies its antiplatelet region

ARTICLE *in* ARCHIVES OF TOXICOLOGY · FEBRUARY 2011

Impact Factor: 5.98 · DOI: 10.1007/s00204-011-0665-6 · Source: PubMed

13 AUTHORS, INCLUDING:

Daniela Priscila Marchi-Salvador
Universidade Federal da Paraíba
27 PUBLICATIONS **215** CITATIONS
SEE PROFILE

Andre Fuly
Universidade Federal Fluminense
56 PUBLICATIONS **973** CITATIONS
SEE PROFILE

Mario Tyago Murakami
Centro Nacional de Pesquisa em Energia e …
119 PUBLICATIONS **1,230** CITATIONS
SEE PROFILE

Suely Vilela Sampaio
University of São Paulo
114 PUBLICATIONS **1,994** CITATIONS
SEE PROFILE

Arch Toxicol
DOI 10.1007/s00204-011-0665-6

MOLECULAR TOXICOLOGY

Molecular characterization of an acidic phospholipase A_2 from *Bothrops pirajai* snake venom: synthetic C-terminal peptide identifies its antiplatelet region

Sabrina S. Teixeira · Lucas B. Silveira · Franco M. N. da Silva · Daniela P. Marchi-Salvador · Floriano P. Silva Jr · Luiz Fernando M. Izidoro · André L. Fuly · Maria A. Juliano · Camila R. dos Santos · Mário T. Murakami · Suely V. Sampaio · Saulo L. da Silva · Andreimar M. Soares

Received: 22 October 2010 / Accepted: 31 January 2011

Abstract This paper describes a biochemical and pharmacological characterization of BpirPLA$_2$-I, the first acidic Asp49-PLA$_2$ isolated from *Bothrops pirajai*. BpirPLA$_2$-I caused hypotension in vivo, presented phospholipolytic activity upon artificial substrates and inhibitory effects on platelet aggregation in vitro. Moreover, a synthetic peptide of BpirPLA$_2$-I, comprising residues of the C-terminal region, reproduced the antiplatelet activity of the intact protein. A cDNA fragment of 366 bp encompassing the mature form of BpirPLA$_2$-I was cloned by reverse transcriptase-PCR of *B. pirajai* venom gland total RNA. A Bayesian phylogenetic analysis indicated that BpirPLA$_2$-I forms a clade with other acid Asp49-PLA$_2$ enzymes from the *Bothrops* genus, which are characterized by the high catalytic activity associated with anticoagulant or hypotensive activity or both. Comparison of the electrostatic potential (EP) on the molecular surfaces calculated from a BpirPLA$_2$-I homology model and from the crystallographic models of a group of close homologues revealed that the greatest number of charge inversions occurred on the face opposite to the active site entrance, particularly in the Ca^{2+} ion binding loop. This observation suggests a possible relationship between the basic or acid character of PLA$_2$ enzymes and the functionality of the Ca^{2+} ion binding loop.

Keywords Snake venom · Acidic phospholipase A_2 · Biochemical and pharmacological characterization · *Bothrops pirajai* · Antiplatelet domain

S. S. Teixeira · L. B. Silveira · F. M. N. da Silva · D. P. Marchi-Salvador · L. F. M. Izidoro · S. V. Sampaio · A. M. Soares
Departamento de Análises Clínicas, Toxicológicas e Bromatológicas, Faculdade de Ciências Farmacêuticas de Ribeirão Preto, FCFRP-USP, Ribeirão Preto, SP, Brazil

D. P. Marchi-Salvador
Departamento de Biologia Molecular, Centro de Ciências Exatas e da Natureza, DBM-UFPB, João Pessoa, PB, Brazil

F. P. Silva Jr
Laboratório de Bioquímica de Proteínas e Peptídeos, Instituto Oswaldo Cruz, IOC-FIOCRUZ, Rio de Janeiro, RJ, Brazil

L. F. M. Izidoro
Faculdade de Ciências Integradas do Pontal, UFU, Ituiutaba, MG, Brazil

A. L. Fuly
Departamento de Biologia Celular e Molecular (GCM), Instituto de Biologia, UFF, Niterói, RJ, Brazil

M. A. Juliano
Departamento de Biofísica, UNIFESP, São Paulo, SP, Brazil

C. R. dos Santos · M. T. Murakami
Laboratório Nacional de Biociências, Centro Nacional de Pesquisas em Energia e Materiais, Campinas, SP, Brazil

S. L. da Silva
Universidade Federal de São João Del Rei, UFSJ Campus, Divinópolis, MG, Brazil

A. M. Soares (✉)
Departamento de Análises Clínicas, Toxicológicas e Bromatológicas, Faculdade de Ciências Farmacêuticas de Ribeirão Preto, Universidade de Sao Paulo—USP, Avenida do Café, s/n°, 14040-903 Ribeirão Preto, SP, Brazil
e-mail: andreims@fcfrp.usp.br

Published online: 18 February 2011

Introduction

Snake venoms are rich in phospholipases A_2 (PLA_2s, EC 3.1.1.4), which induce a large variety of pharmacological and toxic effects, such as myotoxicity, neurotoxicity, cardiotoxicity, hemolysis, hypotension, bleeding, edema, and effects on platelet aggregation (Gutiérrez and Lomonte 1997; Harris et al. 2000; Soares et al. 2004; De Paula et al. 2009).

PLA_2s are enzymes that catalyze the hydrolysis of 2-acyl ester bonds of 3-*sn*-phospholipids producing fatty acids and lysophospholipids. The Ca^{2+} ion, an essential cofactor, and an Asp residue at position 49 are critical points for the catalysis upon artificial substrates (Arni and Ward 1996). There are five types of these enzymes, namely secreted PLA_2s ($sPLA_2$), cytosolic PLA_2s ($cPLA_2$), Ca^{2+} independent PLA_2s ($iPLA_2$), platelet-activating factor acetylhydrolases (PAF-AH), and lysosomal PLA_2s (Schaloske and Dennis 2006).

Snake venom PLA_2s ($svPLA_2$s) are secreted proteins belonging to the groups I and II. The $svPLA_2$s of group I are found in the Elapidae family (Elapinae e Hydrophiinae), whereas those of the group II are found in venoms from Viperidae family (Viperidae e Crotalinae). Usually, the group IIA $svPLA_2$s are divided in two main subgroups: (i) Asp49-PLA_2s, which display an Asp residue at position 49, with relatively high catalytic activity upon artificial substrates; and (ii) Lys49-PLA_2s, showing a Lys residue at position 49, with no catalytic activity (Arni and Ward 1996; Gutiérrez and Lomonte 1997; Ownby et al. 1999; Soares et al. 2004; De Paula et al. 2009).

Acidic PLA_2s isolated from snake venoms have not been fully characterized yet; however, in recent years, the interest in these proteins has increased due to the fact that some enzymes do not present myotoxicity, but induce significant pharmacological effects such as inhibition of platelet aggregation and hypotension (Serrano et al. 1999; Andrião-Escarso et al. 2002; Fuly et al. 2002; Roberto et al. 2004; De Albuquerque Modesto et al. 2006; Fernández et al. 2010).

This paper describes the isolation as well as the biochemical, functional, and structural characterization of the first acidic Asp49-PLA_2 (named BpirPLA_2-I) from *Bothrops pirajai* snake venom and shows that synthetic C-terminal peptide reproduce the antiplatelet effect of the intact protein.

Materials and methods

Materials

Desiccated *B. pirajai* venom was purchased from Bioagents Serpentarium (Batatais, SP, Brazil). Male Swiss mice, weighing 18–25 g, were provided by Biotério Central, Universidade de São Paulo (USP), Ribeirão Preto, SP, Brazil. Animal care was in accordance with the guidelines of the Brazilian College for Animal Experimentation (COBEA) and was approved by the Committee for Ethics in Animal Utilization of Universidade de São Paulo (n°07.1.516.53.6) and IBAMA (n°11781-1). Collagen (Type I) from bovine tendon was purchased from Chrono-Log Corporation, and adenosine diphosphate (ADP) and *p*-bromophenacyl bromide (BPB) were from Sigma Chemical Co. (St. Louis, USA). Fluorescent substrates Acyl 6:0 nitrobenzoxadiazole phospholipids (NBD-phospholipids): NBD-phosphatidylcholine (PC), NBD-phosphatidylglycerol (PG), NBD-phosphatidylethanolamine (PE), or NBD-phosphatidic acid (PA) were from Avanti Polar Lipids Inc. (Alabaster, USA). CM-Sepharose resin was purchased from Amersham Biosciences (Uppsala, Sweden). All other reagents used were of analytical grade.

Purification of BpirPLA_2-I

A 200 mg sample of desiccated *B. pirajai* venom was dissolved in 1.5 ml of 50 mM ammonium bicarbonate (ambic) buffer, pH 7.8, cleared by centrifugation at 480 × *g* for 10 min, and applied on a CM-Sepharose Fast Flow column (2.0 × 20 cm) which was previously equilibrated with the same buffer. A linear gradient was then applied up to 1.0 M NaCl in ambic buffer and fractions of 3.5 ml/tube were collected at a flow rate of 20 ml/h. The fraction with PLA_2 activity (PI-B) was collected and re-chromatographed on a Shimadzu C18 reverse-phase high-performance liquid chromatography (RP-HPLC) column (4.6 × 150 mm), which was equilibrated with solvent A (5% acetonitrile, 0.1% trifluoroacetic acid) and eluted with a concentration gradient of solvent B (60% acetonitrile, 0.1% trifluoroacetic acid) from 30 to 100%, at a flow rate of 1.0 ml/min for 30 min (Andrião-Escarso et al. 2000, 2002). All steps of the purification procedure were carried out at room temperature (25°C). The pure acidic PLA_2 derived from the third RP-HPLC fraction, named Bpir-PLA_2-I, was lyophilized and used for biochemical/pharmacological characterization and amino acid sequence determination.

Biochemical characterization

Polyacrylamide gel electrophoresis (PAGE) was performed in the presence of sodium dodecyl sulfate (SDS–PAGE) following a previously described method (Laemmli 1970). Isoelectric focusing was run according to Vesterberg (1972). Buffalyte, pH range 3.5–9.0 (Pierce, IL), was used to generate the pH gradient. For the N-terminal sequencing, BpirPLA_2-I was dissolved in 0.4 M Tris–HCl buffer, pH

8.1, containing 6 M guanidine-HCl, reduced by DTT (dithiothreitol), and carboxymethylated by iodoacetic acid. A PPSQ-33A (Shimadzu) automatic sequencer was used to identify the amino acid residues in successive rounds of Edman degradation (Rodrigues et al. 2007; Santos-Filho et al. 2008). The molecular mass of BpirPLA$_2$-I was analyzed by MALDI-TOF mass spectrometry using a Voyager-DE PRO MALDI-TOF apparatus (Applied Biosystems, Foster City, CA, USA). The matrix was prepared with 30% acetonitrile and 0.1% TFA and its mass analyzed under the following conditions: accelerate voltage 25 kV, the laser fixed in 2,890 mJ/com2, and continuous acquisition mode, scanning from m/z 6,000–33,000 at a scan time of 5 s. PLA2 band was excised, reduced, alkylated, and submitted to in-gel digestion with trypsin. The peptide mixture was separated by C18 (75 × 100 mm) RP-nano-UPLC (nanoAcquity, Waters) coupled with nano-electrospray on a Q-Tof Ultima mass spectrometer (Waters) at a flow rate of 0.6 µl/min. The gradient was 2–90% (v/v) acetonitrile in 0.1% (v/v) formic acid over 45 min. One MS spectrum was acquired followed by MS/MS of the top three most-intense peaks detected. The spectra was acquired using software MassLynx v.4.1, processed with the software Mascot Distiller v.2.3.2.0, 2009 (Matrix Science Ldt.), and searched against nonredundant protein database (NCBI nr 2009.07.20, 9,298,190 sequences) using engine Mascot v.2.3 (Matrix Science Ltd.).

An automated benchtop simultaneous multiple solid-phase peptide synthesizer (PSSM 8 system from Shimadzu) was used for the solid-phase synthesis of three peptides, corresponding to residues 1–14 (N-pep, NLWQFGKLIMKIAG), 61–71 (M-pep, KIDSYTYSKEN), and 105–117 (C-pep, IKYWFYGAKNCQEK) of BpirPLA$_2$-I (residues 1–15, 70–80 and 115–129 in the common numbering system, respectively). The peptides were synthesized by the Fmoc procedure (Korkmaz et al. 2008). The final peptides were deprotected in TFA and purified by semipreparative HPLC using an Econosil C-18 column (10 μ, 22.5 × 250 mm) and a two-solvent system: (A) trifluoroacetic acid (TFA)/H_2O (1:1,000) and (B) TFA/acetonitrile (ACN)/H_2O (1:900:100). The column was eluted at a flow rate of 5 ml/min with a 10 (or 30)—50 (or 60)% gradient of solvent B over 30 or 45 min. Analytical HPLC was performed using a binary HPLC system from Shimadzu with a SPD-10AV Shimadzu UV–Vis detector, coupled to an Ultrasphere C-18 column (5 μ, 4.6 × 150 mm) which was eluted with solvent systems A_1 (H_3PO_4/H_2O, 1:1,000) and B_1 (ACN/H_2O/H_3PO_4, 900:100:1) at a flow rate of 1.0 ml/min and a 10–80% gradient of B_1 over 20 min. The HPLC column eluates were monitored by their absorbance at 220 nm. The molecular weight and purity of synthesized peptides were checked by MALDI-TOF mass spectrometry (Bruker Daltons) or electrospray LC/MS-2010 (Shimadzu).

Enzymatic activities

Phospholipase A_2 activity was evaluated using three different methods: (a) using egg-yolk emulsion, which contains phosphatidylcholine as substrate (De Haas et al. 1968); (b) the indirect hemolysis on agar gel (Gutiérrez et al. 1988), and (c) using the fluorescent phospholipids NBD-PC, NBD-PA, and NBD-PG as substrates (Rodrigues et al. 2007). The influence of cations was examined in solutions containing 50 mM Tris–HCl, pH 7.5, replacing Ca^{2+} by other divalent ions such as Ba^{2+}, Cu^{2+}, Fe^{2+}, Mg^{2+}, and Zn^{2+} (final concentration 5 mM). For experiments performed in the absence of Ca^{2+}, a final concentration of 10 mM EDTA was used. Finally, the influence of pH was also evaluated by incubating PLA_2 in different buffers (3.5–12.5), then, the enzymatic activity performed as previously described.

Pharmacological activities

Platelet-rich plasma (PRP) was prepared by centrifugation of blood collected from rabbits in citrate (0.31% w/v) at 380 × g at room temperature. Platelet aggregation was measured in a whole blood lumi-aggregometer (Chrono-Log Corporation) (Rodrigues et al. 2007; Santos-Filho et al. 2008). Assays were carried out at 37°C under stirring in siliconized glass cuvettes. Aggregation was triggered with collagen or ADP after preincubation of platelets with isolated PLA_2 or peptides for 2 min. One hundred percent (100%) aggregation was obtained with supramaximal concentration of either collagen or ADP. All experiments were carried out in triplicate.

The hypotensive activity was carried out using male Swiss mice (18 ± 2 g body weight). Arterial pressure was recorded using a noninvasive blood pressure monitoring system (CODA^R, Kent Scientific Corporation) (Fernández et al. 2010). Blood pressure was determined before (0 time) and different times after the intravenous injection of enzyme (15 and 30 µg PLA_2/100 µl PBS). A negative control group received an i.v. injection of 100 µl of PBS alone. The effects of PLA_2 were compared to BPB-modified protein (Andrião-Escarso et al. 2000, 2002).

For the determination of creatine kinase (CK) activity, groups of five male Swiss mice (18–22 g) were injected in the right gastrocnemius muscle with BpirPLA$_2$-I (100 µg/50 µl), PrTX-III (100 µg/50 µl), or PBS alone (50 µl). After 3 h, blood was collected from the tail in heparinized capillary tubes and centrifuged for plasma separation. CK activity was then determined using 4 µl of plasma, which was incubated for 3 min at 37°C with 1 ml of the reagent according to the kinetic CK-UV protocol from Bioclin, Brazil. The activity was expressed in U/L, where one unit

corresponds to the production of 1 mmol of NADH per minute (Santos-Filho et al. 2008).

For the determination of edema-inducing activity, groups of five male Swiss mice (18–22 g) were injected in the subplantar region with the BpirPLA$_2$-I (30 μg/50 μl) or Piratoxin-III (PrTX-III) (30 μg/50 μl) dissolved in PBS. After 30 min, the paw edema was measured with the aid of a low-pressure spring caliper (Mitutoyo-Japan). Zero time values were then subtracted and the differences reported as mean ± S.D. ($n = 5$).

Screening and isolation of the acidic PLA$_2$ cDNA from a venom gland

An adult specimen was killed, its glands removed, and immediately homogenized in liquid nitrogen. After evaporation of the nitrogen, ultra pure TRIZOL LS Reagent, from LIFE Technologies, was used to extract the total RNA. The latter was dissolved in 20 μl of sterile milli-Q water and submitted to RT-PCR step. A pair of specific primers was designed according to the N-terminal sequence, as determined for BpirPLA$_2$-I, and according to the consensus C-terminal sequence obtained from a multiple sequence alignment with other similar svPLA$_2$ (NCBI-GenBank/Swiss Prot). The primers were also designed to add NheI and BamHI restriction sites to facilitate subsequent cloning: PLA-forward: (5′-cgcatatgagcctgtggcaatttgggaag-3′) and PLA-reverse: (5′-gcggatccttagcatggctctgacttctcc-3′). The total RNA (5 μl) was reverse transcribed for 1 h at 42°C using oligo-dt as the primer. The second strand synthesis and amplification of the obtained cDNA was performed by using 2 μl of the above sample and the pair of gene-specific primers in the polymerase chain reaction (PCR). The PCR products were analyzed by means of gel electrophoresis on 1.5% agarose. The gel was stained with ethidium bromide (0.5 mg/ml) and revealed under UV light (Roberto et al. 2004). Purification of the PCR bands was performed using the Concert Rapid PCR Purification System (Gibco BRL) kit, according to the manufacturer specifications. Sequencing was performed using the ABI Prism® Big Dye™Terminator Cycle Sequencing Ready Reaction kit (Perkin Elmer), according to the manufacturer specification. The cDNA sequences corresponding to acidic PLA$_2$s were identified, and the full-length sequence was obtained. The nucleotide sequence was deposited in the GenBank database under accession number GQ406049.

Phylogenetic analysis

Sequences and taxon sampling

Our aim was to include a cross-section of acidic PLA$_2$ enzymes found in the venom of snakes from the Crotalinae and Viperidae subfamilies. A smaller group of basic PLA$_2$ enzymes with known crystal structure from the *Bothrops* genus was also included. As far as possible, we sought to include sequences of at least two species for all but the smallest genera, and representatives of all major clades in the larger genera. The amino acid sequences were obtained from the Swiss-Prot database (*UniProtKB/Swiss-Prot Release 57.5*) by keyword searching and only the regions corresponding to the mature forms of the enzymes were further considered. This preliminary dataset was constrained to the top scoring sequences according to a blast-p comparison with the BpirPLA$_2$-I sequence. In addition, we kept the sequence of the *Echis ocellatus* PLA$_2$ enzyme from the Viperidae subfamily (Eoce1) to serve as the outgroup, leaving the final dataset with 50 sequences (Table 1).

Multiple sequence alignment

Two different multiple sequence alignment (MSA) were obtained within the web servers T-Coffee and MUSCLE (Notredame et al. 2000; Edgar 2004), using program's default parameters. A multiple structural alignment with the snake venom PLA$_2$ structures deposited in PDB (1IJL, 1PSJ, 1U73, 1PP2, 2H8I, 2OQD, 1XXS, 2Q2J, 1QLL, and 1GMZ) was also generated within the CE-MC—Multiple Protein Structure Alignment Server (Guda et al. 2001). This structural alignment was employed in the manual improvement of T-Coffee and MUSCLE alignments in BioEdit v.7.0.5.3 (Hall 1999) using the BLOSUM62 scoring matrix as a visual aid for the generation of the final consensus MSA for subsequent use in the phylogenetic analysis.

Bayesian phylogenetics

Bayesian phylogenetic (BP) analysis was performed with the MrBayes v.3.1.2 program (Ronquist and Huelsenbeck 2003). The amino acid evolution model was estimated from data analysis by determining the contribution of each of the nine different fixed-rate empirical models implemented in MrBayes v.3.1.2 in proportion to their posterior probabilities. The parameter for the "rate variation across sites" was set to 'invgamma' (i.e., rates vary over sites according to a gamma distribution while allowing a proportion of sites to be invariable). One cold and three heated Markov chain Monte Carlo (MCMC) chains with default chain temperatures were run in each of two simultaneous runs (starting from different random trees) for 1.0×10^6 generations, sampling log-likelihood values, and trees at 100-generation intervals. The first 2.5×10^5 generations (i.e., 2,500 trees) were discarded in the analyses as "burn-in" with a generous "safety margin". Plots of ln(L) against

Table 1 Description of taxa along with individual identifiers, PDB codes and Swiss-Prot accession numbers snake venom PLA_2 enzymes from the Viperidae family. Enzymes from the Crotalinae subfamily were further divided on acid and basic PLA_2

Species	Individual identifier	PDB code	Swiss-Prot accession number
Viperinae			
Echis ocellatus	Eoce1		B5U6Y5
***Crotalinae*—acidic PLA_2**			
Agkistrodon acutus (*Denagkistrodon acutus*)	Aacu1	1IJL	Q7SID6
Agkistrodon halys blomhoffi (*Gloydius blomhoffi*)	Ahbl1		P20249
Agkistrodon halys pallas (*Gloydius halys pallas*)	Ahpa1	1PSJ	P14418
Agkistrodon halys pallas (*Gloydius halys pallas*)	Ahpa2		O42189
Agkistrodon halys pallas (*Gloydius halys pallas*)	Ahpa3		O42190
Agkistrodon halys pallas (*Gloydius halys pallas*)	Ahpa4		O42191
Agkistrodon halys pallas (*Gloydius halys pallas*)	Ahpa5		O42192
Agkistrodon rhodostoma (*Calloselasma rhodostoma*)	Arho1		Q9PVF2
Bothriechis schlegelii	Bsch1		A8E2V4
Bothrops erythromelas	Bery1		Q2HZ28
Bothrops insularis	Bins1		Q8QG87
Bothrops jararaca	Bjar1		P81243
Bothrops jararacussu	Bjus1	1U73	Q8AXY1
Bothrops pictus	Bpic1		Q9I8F8
Bothrops pirajai	BpirPLA_2-I		GQ406049[a]
Cerrophidion godmani (*Bothrops godmani*)	Cgod1		A8E2V5
Cerrophidion godmani (*Bothrops godmani*)	Cgod2		A8E2V6
Crotalus adamanteus	Cada1		P00623
Crotalus atrox	Catr1	1PP2	P00624
Crotalus viridis viridis	Cvvi1		Q7ZTA7
Gloydius shedaoensis (*Agkistrodon shedaoensis*)	Gshe1		Q6T5K9
Gloydius ussuriensis (*Agkistrodon caliginosus*)	Guss1		Q7LZQ4
Lachesis stenophrys	Lste1		P84651
Sistrurus catenatus tergeminus	Scte1		Q2TU95
Trimeresurus elegans (*Portobothrops elegans*)	Tele1		Q2PG83
Trimeresurus flavoviridis (*Protobothrops flavoviridis*)	Tfla1		P06859
Trimeresurus flavoviridis (*Protobothrops flavoviridis*)	Tfla2		Q92147
Trimeresurus gracilis	Tgra1		A8E2V8
Trimeresurus gramineus	Tgrm1		P20476
Trimeresurus gramineus	Tgrm2		P81478
Trimeresurus gramineus	Tgrm3		P81480
Trimeresurus gramineus	Tgrm4		P81479
Trimeresurus gramineus	Tgrm5		P70088
Trimeresurus mucrosquamatus (*Protobothrops mucrosquamatus*)	Tmuc1		Q91506
Trimeresurus okinavensis (*Ovophis okinavensis*)	Toki1		P00625
Trimeresurus puniceus	Tpun1		Q2YHJ5
Trimeresurus stejnegeri (*Viridovipera stejnegeri*)	Tste1		P82896
Trimeresurus stejnegeri (*Viridovipera stejnegeri*)	Tste2		Q6H3D0
Trimeresurus stejnegeri (*Viridovipera stejnegeri*)	Tste3		Q6H3C7
Trimeresurus stejnegeri (*Viridovipera stejnegeri*)	Tste4		Q6H3C9
Trimeresurus stejnegeri (*Viridovipera stejnegeri*)	Tste5		Q6H3C8
***Crotalinae*—basic PLA_2**			
Bothrops jararacussu	Bju_1	2H8I	Q90249
Bothrops jararacussu	Bju_2	2OQD	P45881
Bothrops moojeni	Bmo_1		P82114

Table 1 continued

Species	Individual identifier	PDB code	Swiss-Prot accession number
Bothrops moojeni	Bmo_2	1XXS	Q9I834
Bothrops moojeni	Bmo_3		P0C8M1
Bothrops pirajai	Bpi_1	2Q2J	P58399
Bothrops pirajai	Bpi_2	1QLL	P82287
Bothrops pirajai	Bpi_3	1GMZ	–

Not all the snake venom PLA_2s already isolated are shown

[a] GenBank accession number

generation were inspected to check the appropriateness of the burn-in period. Bayesian posterior probabilities (BPP) and branch lengths were calculated from the remaining trees, which were finally summarized as an extended majority-rule consensus tree carrying the posterior probabilities at the different nodes. MrEnt version 2.0 (Zuccon and Zuccon 2008) was used for tree viewing and editing.

Comparative modeling

Modeling of the BpirPLA$_2$-I three-dimensional structure was performed by the method of satisfaction of spatial restraints implemented in the program Modeller 9v6 (Sali and Blundell 1993). A model was constructed for the Ca^{2+}-free (apo form) of BpirPLA$_2$-I. The model was constructed using different crystal structures of an acid PLA_2 from the *B. jararacussu* venom (BthA-I-PLA$_2$) as templates to average out uncertainties or artifacts in the atomic coordinates coming from surface loop flexibility as well as crystal packing effects and other technical issues: 1ZLB (0.97 Å resolution), chains A and B of 1U73 (1.90 Å resolution), and 1UMV (1.79 Å resolution). The sequence alignment between the multiple templates and BpirPLA$_2$-I was trivial due to the high sequence identity shared between BpirPLA$_2$-I and BthA-I-PLA$_2$ (90%) and could be visually adjusted. Five models were generated, and the model with the lowest value of the Modeller objective function was selected for further evaluation and validation. The presence of any energetically unfavorable regions in the model was evaluated with the Discrete Optimized Protein Energy function (DOPE) (Shen and Sali 2006) by comparing the DOPE score profile of the templates. External assessment of the stereochemical quality and overall structural reliability of the model was performed within the Structural Analysis and Verification Server (SAVES) at the WWW address http://nihserver.mbi.ucla.edu/SAVES/.

Electrostatic potential calculations

The electrostatic surface potentials (EP) for BpirPLA$_2$-I and its homologs—BthA-I-PLA$_2$ (pdb code 1U73), PrTX-III (pdb code 1GMZ), and PrTX-I (pdb code 2Q2J) were calculated from the 3D atomic coordinates of the free PLA_2 enzymes by solving the Poisson − Boltzmann equation using the program DelPhi v.4 (Rocchia et al. 2001) with charge parameters from the CHARMM force field (MacKerell et al. 1998) and atom radii parameters from PARSE (Sitkoff et al. 1994a, b). Hydrogen atoms were added using the Biopolymer module from the Sybyl v.8.0 software package (Tripos Inc., St. Louis, MO, USA). Since hydrogen addition may add structural crushes, for each structure, 100 steps of minimization for relaxing added hydrogen atoms were performed to obtain the structures that were used in the electrostatic calculations.

Statistical analysis

Results are presented as the mean value ± SD obtained with the indicated number of animals or samples. The statistical significance of differences between groups was evaluated using Student's unpaired *t* test and analysis of variance (ANOVA). A P value <0.05 was considered to indicate significance.

Results and discussion

Several snake venoms were fractionated using procedures based on ion exchange and hydrophobic interaction chromatography for phospholipases A_2 purification (Gutiérrez and Lomonte 1997; Ownby et al. 1999; Andrião-Escarso et al. 2000; Soares et al. 2004; De Paula et al. 2009). Purification of BpirPLA$_2$-I from *Bothrops pirajai* snake venom was achieved by ion exchange chromatography on CM-Sepharose, resulting in seven major peaks (Fig. 1a). Fraction P-Ib with high phospholipase A_2 activity was subjected to RP-HPLC (resin C18/acetonitrile-TFA) to remove traces of other components of the venom (Fig. 1b). The active PLA_2, called BpirPLA$_2$-I, was obtained as a well-resolved sharp peak eluting at approximately 40% acetonitrile (Fig. 1c). The purified protein sample was observed as single bands of M_r around 14 kDa and

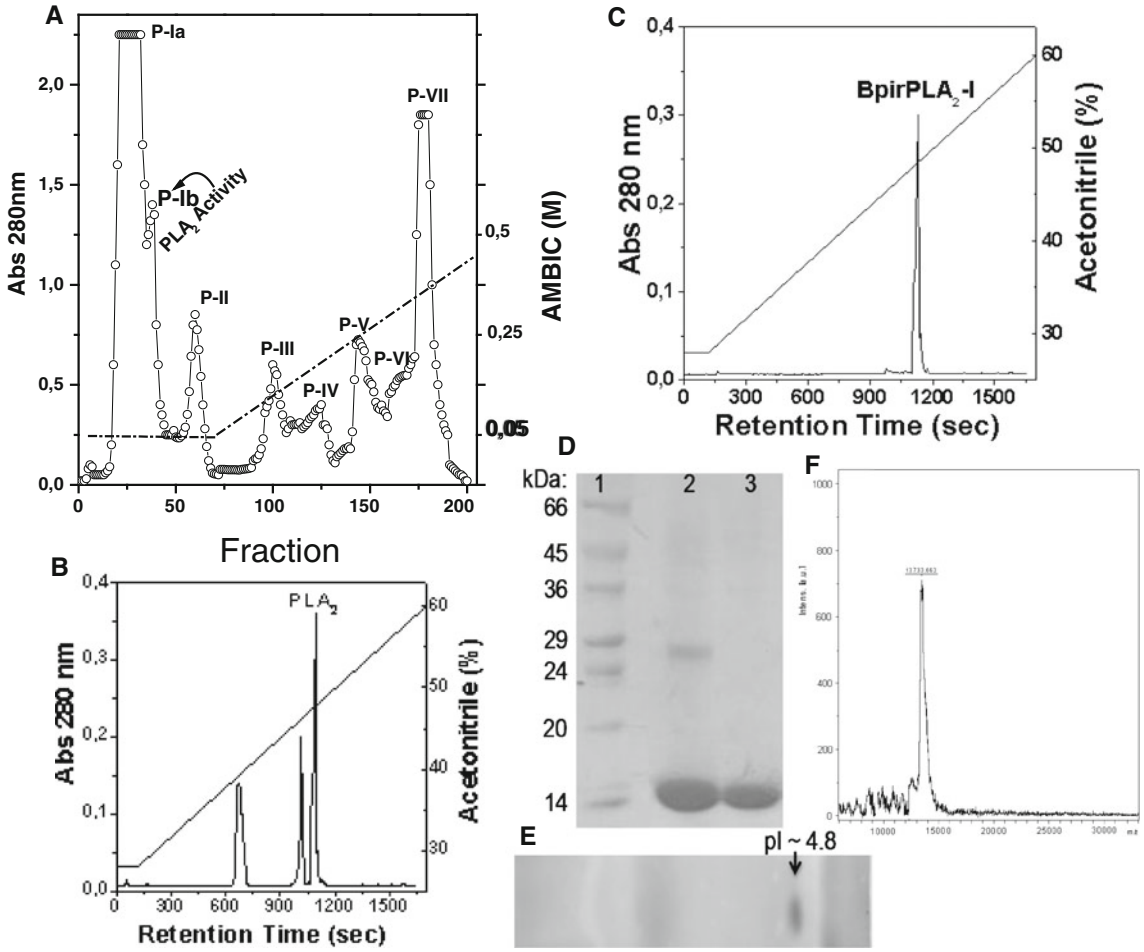

Fig. 1 Isolation of acidic PLA_2 from *Bothrops pirajai* snake venom. **a** ion exchange chromatography on CM-Sepharose of 200 mg of *Bothrops pirajai* venom. The fractions were identified as P-I to P-VII. The sample was eluted with buffer in a linear gradient of ammonium bicarbonate (0.05–1.0 M), at a flow rate of 20 ml/h, collecting fractions up to 3.5 ml/tube. **b** Chromatographic profile obtained from a reverse-phase C18 HPLC. The sample 10 mg of P-Ib was eluted using solvent A (5% acetonitrile, 0.1% TFA) in the concentration gradient of 30–100% of solvent B (acetonitrile 60%, TFA 0.1%), with a flow of 1 ml/min for 70 min. **c** Assessment of purity of RP-HPLC under the same conditions. Electrophoretic analysis to verify the homogeneity of the acidic phospholipase A_2, $BpirPLA_2$-I, isolated from the venom of *B. pirajai*. **d** 12% SDS–PAGE. Samples: 1-MWM, 2- nonreduced $BpirPLA_2$-I (30 μg), 3- reduced $BpirPLA_2$-I (30 μg). **e** Isoelectric focusing: pI ∼ 4.8 for $BpirPLA_2$ was determined using the method previously described (see "Materials and methods" section). **f** Mass determination of $BpirPLA_2$-I by mass spectrometry (see "Materials and methods" section)

13,733.6 in the reducing SDS–PAGE (Fig. 1d) and MS (Fig. 1f), respectively. Under native PAGE for acidic proteins, the purified $BpirPLA_2$-I sample also consisted of a single band migrating toward to the positive pole (data not shown), which was in agreement with the isoelectric point of 4.8 determined from IEF (Fig. 1e).

The acidic PLA_2 from *B. pirajai* showed higher enzymatic activity compared to PrTX-III, a basic Asp49-PLA_2 from the same venom (data not shown). These results are in agreement with previous studies involving PLA_2s of snake venom, in which the acidic Asp49-PLA_2s are catalytically more active than their basic isoforms (Andrião-Escarso et al. 2002; Roberto et al. 2004; Rodrigues et al. 2007; Santos-Filho et al. 2008; Fernández et al. 2010).

The phospholipase activity of $BpirPLA_2$-I was dose dependent (Fig. 2a), and the enzyme was stable even when subjected to extreme temperatures (4–100°C) and pH values (2.5–10) (Fig. 2b, c). However, the treatments with EDTA and BPB (inhibitor of PLA_2s) inhibited the phospholipase activity of the protein. The inhibition of enzymatic activity in the presence of EDTA is in accordance with the need for divalent ions as cofactors for the catalytic activity, as shown for other homologous enzymes (Gutiérrez and Lomonte 1997; Soares et al. 2004). The alkylation process of the His48 residue by preincubation of $BpirPLA_2$-I with BPB completely abolished such activity (Fig. 2f). This difference may be related to a possible distortion in the calcium binding loop, as observed by

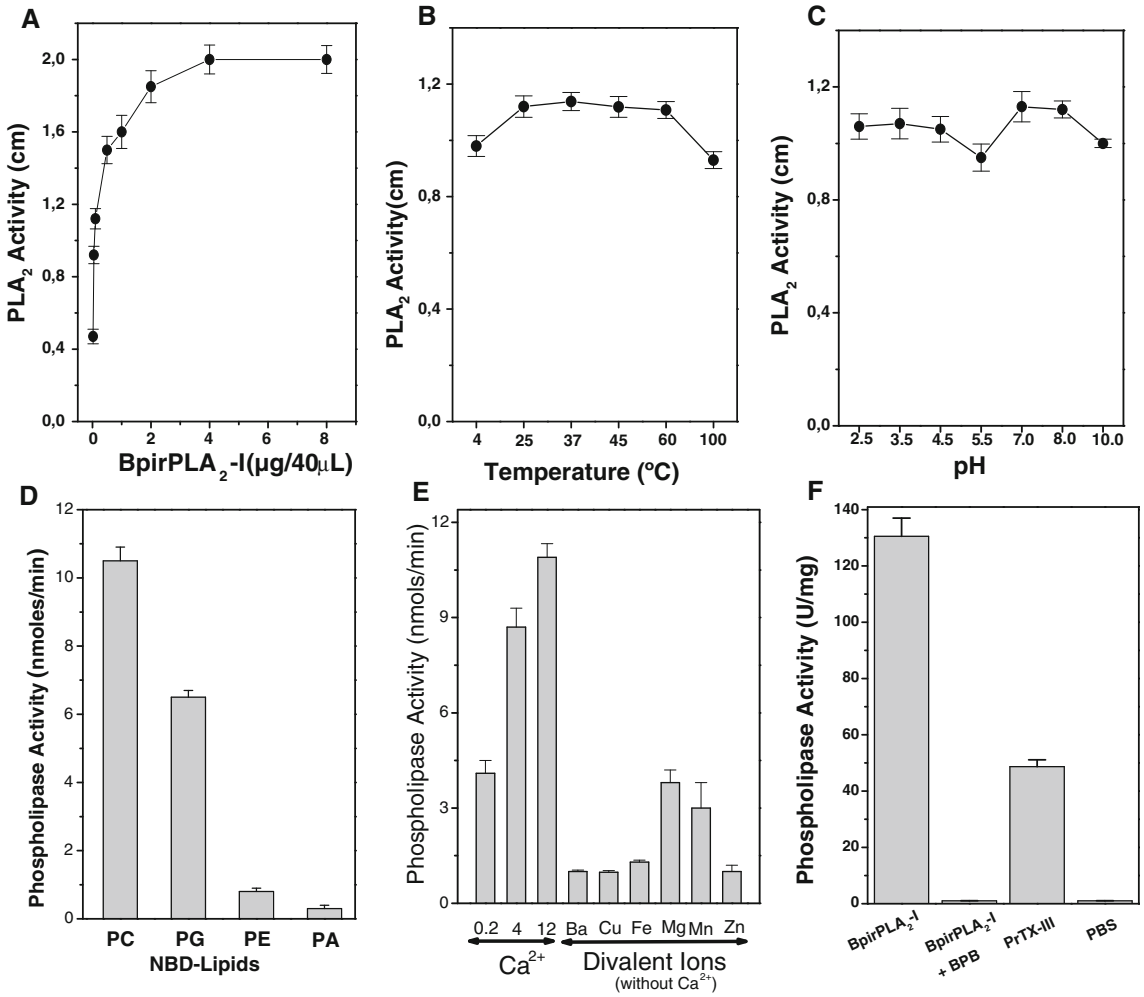

Fig. 2 Enzymatic characterization of BpirPLA$_2$-I. The phospholipase A$_2$ activity was measured by three different methods (hemolysis, fluorescent lipids, and egg-yolk emulsion). *Indirect hemolysis* (express in centimeters): **a** PLA$_2$ activity and variation of enzyme concentration, **b** PLA$_2$ activity and temperature variation, **c** PLA$_2$ activity and changes in pH. *Fluorescent lipids* (1U was considered as the amount in micrograms of enzyme that releases the product in nmol per minute): **d** PLA$_2$ activity of BpirPLA$_2$-I (15 µg/ml) on fluorescent phospholipids NBD-PC (phosphatidylcholine), NBD-PA (phosphatidic acid), NBD-PG (phosphatidylglycerol), and NBD-PE (phosphatidylethanolamine). **e** PLA$_2$ activity of BpirPLA$_2$-I (10 µg/ml) on NBD-PC in the presence of different divalent ions. *Egg-yolk emulsion* (express in U/mg enzyme): **f** PLA$_2$ activity of BpirPLA$_2$-I (25 µg) in the presence and absence of BPB inhibitor. *B. pirajai* PrTX-III (50 µg) and PBS were used as control. The results were expressed as mean ± SD ($n = 3$)

Correa and coworkers (2008) in a comparative structural study carried out with different phospholipases A$_2$.

BpirPLA$_2$-I hydrolyzed fluorescent phospholipids such as NBD-PC and NBD-PG with different rates (Fig. 2d), showing to be more active upon NBD-PC, similar to the acidic PLA$_2$s BmooTX-I and Bp-PLA$_2$, purified from *B. moojeni* and *B. pauloensis* snake venoms, respectively (Rodrigues et al. 2007; Santos-Filho et al. 2008). Hence, NBD-PC was used to study the influence of metals on BpirPLA$_2$-I activity. The presence of calcium ions increased the activity of PLA$_2$ in a dose-dependent manner, unlike the other tested divalent ions (Ba^{+2}, Cu^{+2}, Fe^{+2}, Mg^{+2}, Mn^{+2}, and Zn^{+2}) (Fig. 2e). In catalytically active PLA$_2$s, a Ca^{+2} ion, coordinated by Asp49 residue, a water molecule, and oxygen atoms of residues Gly30, Gly32, and Trp31 are responsible for stabilizing the reactive intermediate (Arni and Ward 1996). In the absence of calcium, a water molecule occupies the position of the ion and the side chain of Asp49 residue and the calcium binding loop adopt different conformations, affecting the enzymatic activity (Murakami et al. 2006). Thus, these results are consistent with the characteristics of PLA$_2$s that include high stability, due to large number of intrachain disulfide bridges, and the need for calcium as a cofactor for the enzymatic activity.

BpirPLA$_2$-I is a new antiplatelet agent, inducing aggregation inhibition of platelet-rich plasma (PRP) in a dose-dependent manner, promoted by ADP (Fig. 3a) or collagen (Fig. 3b). The effect of BpirPLA$_2$-I upon human

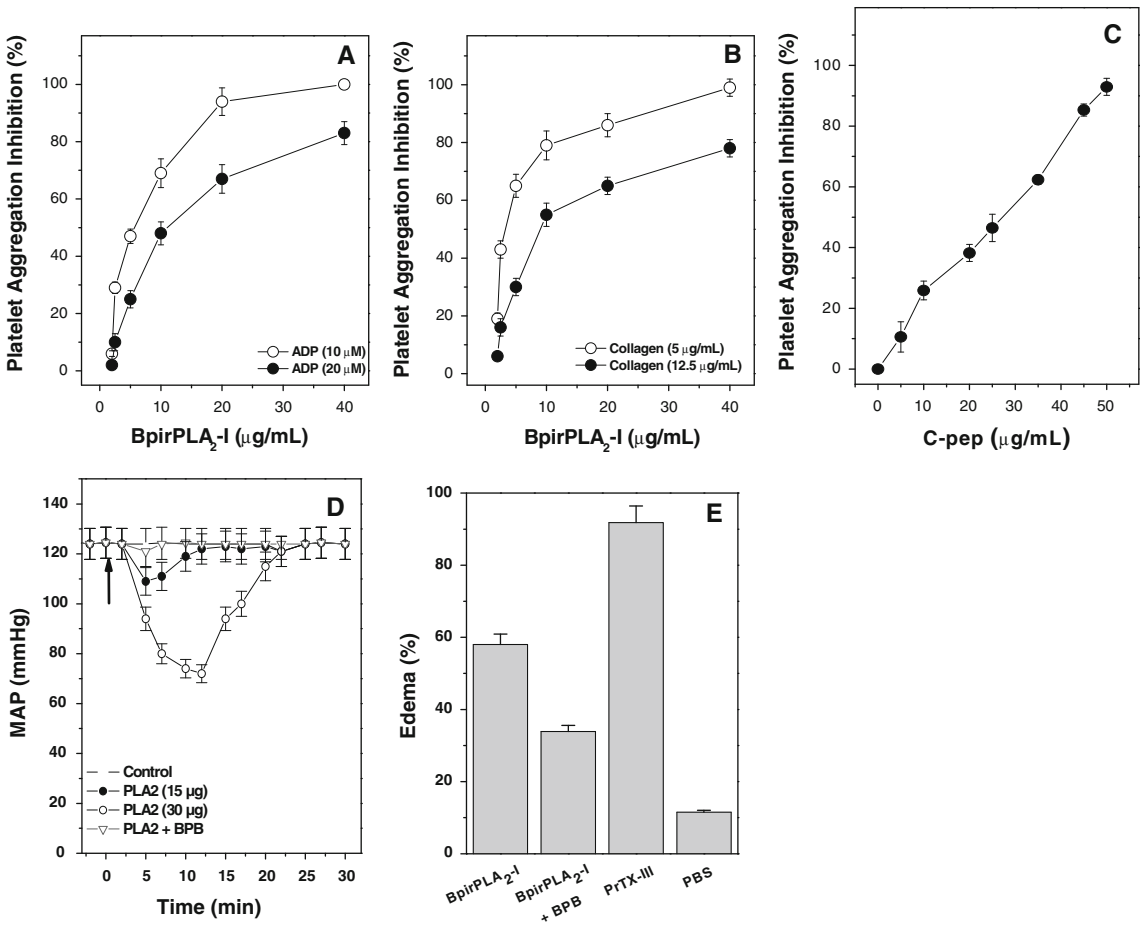

Fig. 3 Pharmacological characterization of BpirPLA$_2$-I. Inhibition of platelet aggregation induced by BpirPLA$_2$-I in the presence of ADP **(a)** or collagen **(b)**. The enzyme activity was evaluated on platelet-rich plasma (PRP). **c** C-pep (5–50 μg/ml) was preincubated with platelets at 37°C under stirring for 2 min, and then collagen (5 μg/ml) was added to trigger aggregation. Maximal aggregation was achieved 6 min after adding collagen and compared with values obtained in the presence of C-pep. Data are expressed as means ± SD of two individual experiments ($n = 3$). **d** Hypotensive activity of BpirPLA$_2$-I (*arrow*) on blood pressure. Note the abolishment of hypotensive activity in the administration of the enzyme previously modified with BPB. **e** Analysis of the edematogenic activity of BpirPLA$_2$-I (30 μg) in mice. Edema was measured 30 min after subplantar injection of PLA$_2$s. The results were expressed as mean ± SD ($n = 5$)

platelet aggregation was also investigated. The same data were observed for human platelets (data not shown). Several studies involving acidic PLA$_2$s, BthA-I-PLA$_2$ from *B. jararacussu* (Andrião-Escarso et al. 2002; Roberto et al. 2004), BE-I-PLA$_2$ from *B. erythromelas* (De Albuquerque Modesto et al. 2006), LM-PLA2-II from *Lachesis muta* (Fuly et al. 2002), and TJ-PLA$_2$ from *Trimeresurus jerdonii* (Lu et al. 2002) demonstrated the inhibitory effect of these enzymes on platelet aggregation. A synthetic C-terminal peptide (C-pep) reproduced the antiplatelet activity of the intact BpirPLA$_2$-I protein (Fig. 3c). On the other hand, synthetic N- and M-peptides did not have any effect on platelet aggregation (data not shown). Therefore, for the first time, it was demonstrated that the C-terminal region, which comprises a relatively short stretch of amino acids (115–129) near the C-terminal loop, plays an important role in the antiplatelet activity induced by a svPLA$_2$. Although the C-pep has reproduced the antiplatelet activity of the intact BpirPLA$_2$-I, we do not discard the participation of the catalytic region in this activity. As observed in the literature, the antiplatelet activity of some p-BPB-modified PLA$_2$ isolated from *B. jararacussu* (Andrião-Escarso et al. 2002), *B. erythromelas* (De Albuquerque Modesto et al. 2006), *L. muta* (Fuly et al. 2002), and *B. moojeni* (Santos-Filho et al. 2008) snake venoms was affected. The inhibitory effect of BpirPLA$_2$-I on platelet aggregation was also abolished after treatment with p-BPB (data not shown).

It is well known that only the His48 residue is chemically modified by the *p*-bromophenacyl bromide (Andrião-Escarso et al. 2000; Soares and Giglio 2003; Soares et al. 2004; Marchi-Salvador et al. 2009). This alkylation occurs in the imidazole ring (Nδ1 atom) of the His48 residue present in the active site and promotes the loss of the

enzymatic activity and/or reduction in the toxic and pharmacological effects of PLA_2s (Soares et al. 2004). This suggests that these pharmacological effects and the catalytic activity are dependent on His48. Marchi-Salvador and coworkers (2006) suggested that the inhibitor binding led to significant structural modifications, especially in the C-terminal region. In the structure of BthTX-I, a Lys49 phospholipase A_2 like from *Bothrops jararacussu*, chemically modified with BPB, it was observed that the phenacyl group of BPB molecule extends along the hydrophobic channel of the protein, interacting with Tyr22, Gly23, Val31, Cys45, and Lys49 residues.

Another PLA_2 isolated from *Bothrops jararacussu* venom, named BthA-I, was also complexed with BPB, and it was observed that the catalytic, platelet-aggregation inhibition, anticoagulant, and hypotensive activities were abolished by ligand binding. The BthA-I-BPB complex contains three structural regions that are modified after inhibitor binding: the Ca^{2+}-binding loop, beta-wing, and C-terminal regions. This conformation is more energetically and conformationally stable than the native structure, and the abolition of pharmacological activities by the ligand may be related to the oligomeric structural changes (Magro et al. 2005).

BpirPLA$_2$-I induced hypotension in rats. This activity was completely abolished in the presence of BPB (Fig. 3d). The synthetic peptides did not have any effect on hypotension. Up to now, there is no structural information, suggesting the presence of a pharmacological site on phospholipases A_2 associated with the hypotensive effect of these enzymes. According to Huang and Lee (1984), the activity of hypotensive PLA_2s must be related to the synthesis of prostaglandins from the molecule of arachidonic acid (AA) released by the phospholipase A_2 catalytic activity. These prostaglandins act on the renin-angiotensin system, a set of protein molecules involved in controlling the volume of extracellular fluid and blood pressure. In addition, the leukotrienes, also derived from AA by the action of lipoxygenase, could attend acting on the smooth muscle of blood vessels.

Synthetic peptides have been studied in order to find out which regions of the snake venoms phospholipases A_2 are responsible for each activity (Lomonte et al. 2010). A synthetic peptide derived from a homologue PLA_2 present in *Bothrops asper* snake venom has shown potent bactericidal activity and exerts potent fungicidal activity against a variety of clinically relevant *Candida* species (Murillo et al. 2007). Costa and coworkers (2008) also demonstrated that cationic synthetic peptides derived from the 115–129 C-terminal region of myotoxic PLA_2s from *Bothrops brazili* snake venom, MTX-I (Asp49 PLA_2) and MTX-II (Lys49 PLA_2), displayed cytotoxic activity on human T-cell leukemia (JURKAT) lines and microbicidal effects against *Escherichia coli*, *Candida albicans*, and *Leishmania* sp. The in vitro and in vivo antitumor activity of a cationic synthetic peptide was derived from the 115–129 C-terminal region of BPB-modified BthTX-I (Gebrim et al. 2009). Up to now, the toxic activities of these PLA_2s have been attributed to its C-terminal region.

The intradermal administration of 30 μg of BpirPLA$_2$-I was able to induce edema (increase of 58% in rat paw volume), which was reduced by 34% after preincubation of enzyme with BPB (Fig. 3e). In contrast, the same amount of PrTX-III induced edema of 92%. These results are in agreement with previous studies with *B. jararacussu* acidic PLA_2s where the chemical modification with BPB completely eliminated the enzymatic, anticoagulant and antiplatelet activity, but only partially inhibited the formation of edema (Andrião-Escarso et al. 2002; Ketelhut et al. 2003), indicating that in addition to a preserved catalytic site, specific pharmacological requirements seem to be involved with this activity. BpirPLA$_2$-I did not increased CK levels, not showing myotoxicity (results not shown), corroborating with previous findings in which acidic PLA_2s, although highly catalytic active, usually do not have toxicity (Andrião-Escarso et al. 2002; De Albuquerque Modesto et al. 2006; Fernández et al. 2010), dissociating the catalytic activity from myotoxicity. The BpirPLA$_2$-I and synthetic peptides showed very low cytotoxic activity in vitro on skeletal muscle (C_2C_{12}) cells when compared with the synthetic C-terminal region peptides of basic PLA_2s (data not shown).

BpirPLA$_2$-I represents 2–3% of the whole venom being the most abundant acidic PLA_2 in this snake venom and presenting a series of important pharmacological effects such as edema inducing hypotensive and inhibition of platelet aggregating activity.

Amplification and cloning of the BpirPLA$_2$-I cDNA isolated from the venom gland of *B. pirajai* disclosed a fragment with total length of 366 base pairs that encodes a mature PLA_2 enzyme of 122 amino acid residues (Fig. 4), as observed with several other PLA_2 enzymes (Serrano et al. 1999; Ownby et al. 1999; Soares et al. 2004).

A Bayesian phylogenetic (BP) analysis of PLA_2 protein sequences from the Viperidae family was carried out to investigate the evolutionary relationships between BpirPLA$_2$-I and groups of snake venom PLA_2 enzymes having distinct structural (Asp49 vs Lys49), physical–chemical (basic vs acid), and functional features (myotoxic, anticoagulant, hypotensive, neuromuscular transmission blocking as well as measurable PLA_2 catalytic activity). The BP analysis was performed on the PLA_2 dataset (50 taxa; 128 characters) under an EMP + Γ + I model, where EMP is a composition of nine empirical models of protein sequence evolution implemented in the MrBayes code, with each model contributing in proportion to its Bayesian posterior

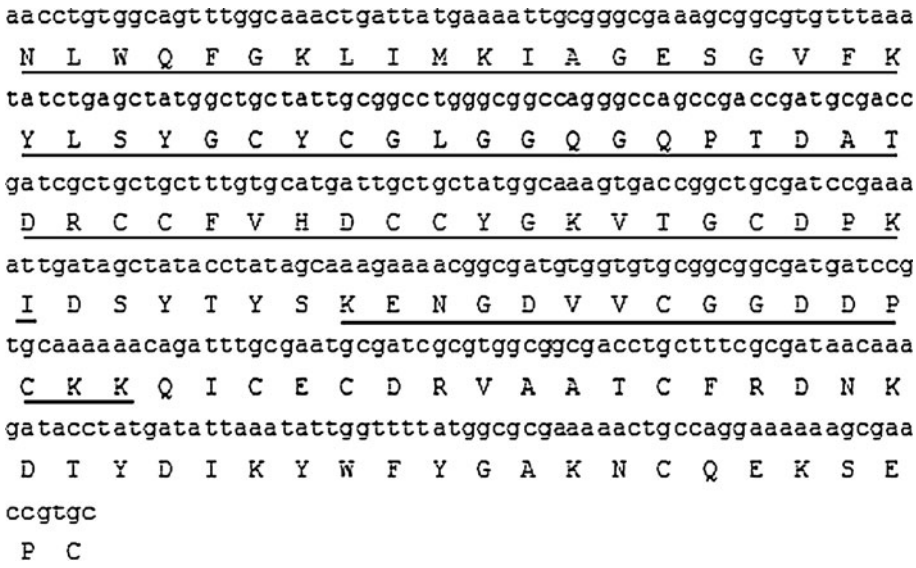

Fig. 4 cDNA sequence and deduction of the amino acid sequence of BpirPLA$_2$-I. The N-terminal sequence and the tryptic peptides of BpirPLA$_2$-I were confirmed by direct sequencing and by ESI-CID-MS/MS, respectively (*underlined*)

probability. For the PLA$_2$ dataset, the maximum likelihood improvement of the JTT matrix (Gonnet et al. 1992; Jones et al. 1992), known as the WAG matrix (Whelan and Goldman 2001), was the single model supported by the data, with a BPP of 1.0.

The BP analysis supported a majority-rule consensus tree (Fig. 5) with a major division between acid and basic PLA$_2$ enzymes. Although the net charge of a protein at physiological pH can be altered with a few amino acid substitutions, the result of the BP analysis for svPLA$_2$ enzymes indicates that divergence of basic (positively charged) and acid (negatively charged) was an early event in the evolution of this protein family. These results corroborate several previous studies on the evolution of svPLA$_2$ enzymes (Ogawa et al. 1996; Valentin and Lambeau 2000; Ohno et al. 2003). At least in the case of species within the *Bothrops* genus, this likely duplication event has originated paralogous genes encoding enzymes with a clearly distinct range of biological activities. For instance, most of the basic PLA$_2$ enzymes have moderate or undetectable catalytic activity but show myotoxic and neuromuscular transmission blocking activities. On the other hand, acid PLA$_2$ enzymes present high catalytic activity associated with anticoagulant or hypotensive activity or both. An exception is Bins1, a PLA$_2$ from *B. insularis* venom (Cogo et al. 2006), which blocks neuromuscular transmission and is myotoxic unlike the other acid PLA$_2$ enzymes from the *Bothrops* genus.

As expected, BpirPLA$_2$-I formed a clade with other acid Asp49-PLA$_2$ enzymes and was shown to be closely related to the PLA$_2$ from *B. jararacussu* (Bjus1), *B. jararaca* (Bjar1), and *B. insularis* (Bins1) with high BPP support values. Interestingly, Bjar1 and Bins1 form a subgroup. Bins1 is distinguished by its myotoxic and neuromuscular transmission blocking activities, which still must be demonstrated to exist in Bjar1 (Serrano et al. 1999).

Within the basic PLA$_2$ clade, another important diversification is associated with the mutation resulting in the substitution of the Asp49 for Lys. This distinct group of enzymes is characterized in the functional level by the absence of any measurable PLA$_2$ catalytic activity. The sequence alignment in the right panel of Fig. 5 clearly shows that many other amino acid substitutions accompany the Asp49 for Lys mutation within the basic *Bothrops* sp. PLA$_2$ clade. This alignment also brings into attention the structural diversity in the N-terminal half of the snake venom PLA$_2$ enzymes. Remarkably, a small set of alignment positions was sufficient to explain most of the branching pattern for the *Bothrops genus* in the BP tree: 10, 18–20, 22–23, 33, 46, 49.

Comparative molecular modeling was employed to predict the 3D structure of BpirPLA$_2$-I based on the similarity of its amino acid sequence to PLA$_2$ enzymes with known 3D structures. The BpirPLA$_2$-I 3D model with lowest DOPE score was subjected to external validation within the SAVES server. The model presented acceptable stereochemical quality with 95.1 and 4.9% of the residues in the most favored and additionally allowed regions of the Ramachandran plot generated within ProCheck software (Laskowski et al. 1993). Furthermore, all residues in the BpirPLA$_2$-I 3D structure presented an averaged 3D-1D score >0.2 within the Verify-3D software (Bowie et al. 1991; Luthy et al. 1992). Hence, this theoretical BpirPLA$_2$-I 3D model was considered satisfactory for the purposes of our analysis.

As expected, the BpirPLA$_2$-I 3D model presented all the general structural features of the snake venom PLA$_2$ family (Correa et al. 2008; Marchi-Salvador et al. 2008, 2009; Dos Santos et al. 2009). The active site is formed by the

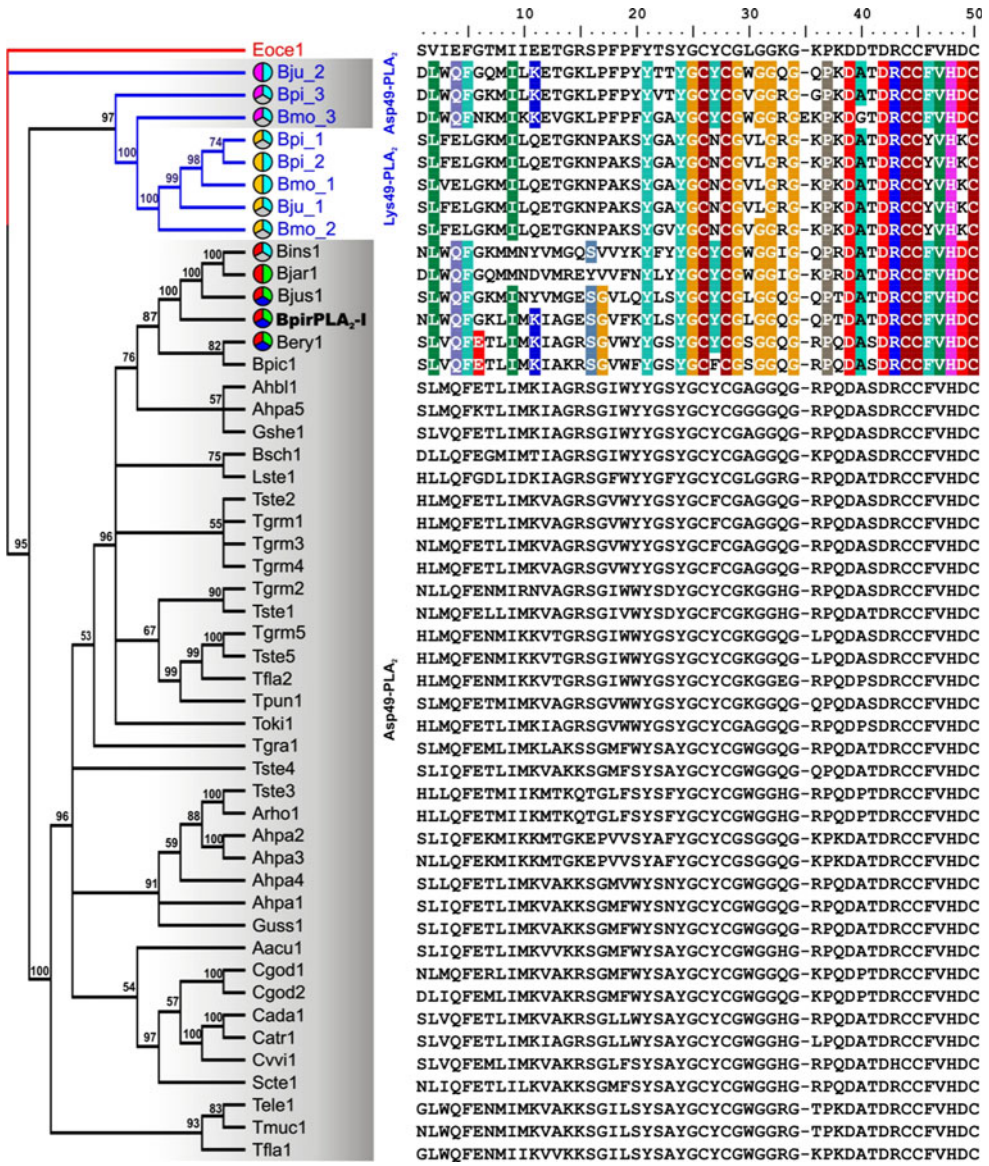

Fig. 5 Bayesian phylogenetic (BP) analysis of BpirPLA$_2$-I homologues in the snake venoms from the Viperidae family. A list of Swiss-Prot accession numbers and Protein Data Bank codes (where applicable) is provided for these proteins and their unique identifiers in Table 1, along with the scientific names of their species. A majority-rule consensus BP tree was inferred from the PLA$_2$ dataset (50 taxa; 128 characters) under the WAG + Γ + I model (the WAG fixed-rate model of protein evolution was estimated from data with BP probability (BPP) of 1.0). BPPs are shown above branches supported with values >50%. The red branch detaches the outgroup from the Viperidae subfamily, an acid PLA$_2$ from *Echis Ocellatus* venom. The blue branches mark the basic PLA$_2$ enzymes from the *Bothrops* genus. Asp49-PLA$_2$ enzymes are highlighted by a *gray* background. The colored pie charts accompanying the unique identifiers for *Bothrops* sp. PLA$_2$ sequences summarize the available functional data for these enzymes: *yellow*—no measurable PLA$_2$ catalytic activity; *magenta*—moderate PLA$_2$ catalytic activity (i.e., ~6-fold lower activity than acid PLA$_2$ enzymes); *red*—high PLA$_2$ catalytic activity; *cyan*—myotoxic activity; *green*—anticoagulant activity; *blue*—hypotensive activity; and *gray*—neuromuscular transmission blockage. On the *right* panel is shown the first 50 positions of the multiple sequence alignment used in the phylogenetic analysis in order to highlight the structural features responsible for the observed branching pattern in the tree. For the *Bothrops* sp. sequences, the conserved positions in the alignment were *shaded* according to physico-chemical properties of the amino acids (color figure online)

residues His48, Asp49, Tyr52, and Asp99 found in the α-helixes "h2" and "h3". Nested between the region known as the β-wing and the active site is the N-terminal α-helix ("h1", residues 1–12) that is involved in the binding and proper orientation of substrates to the catalytic apparatus through a hydrophobic channel. To the right of the active site is located the C-terminal loop (residues 108–133). Just behind the active site is found the Ca^{2+} ion binding loop formed by residues ($C_{27}XCGXGG_{33}$) (Arni and Ward 1996). The residues have been numbered according to Renetseder et al. 1985.

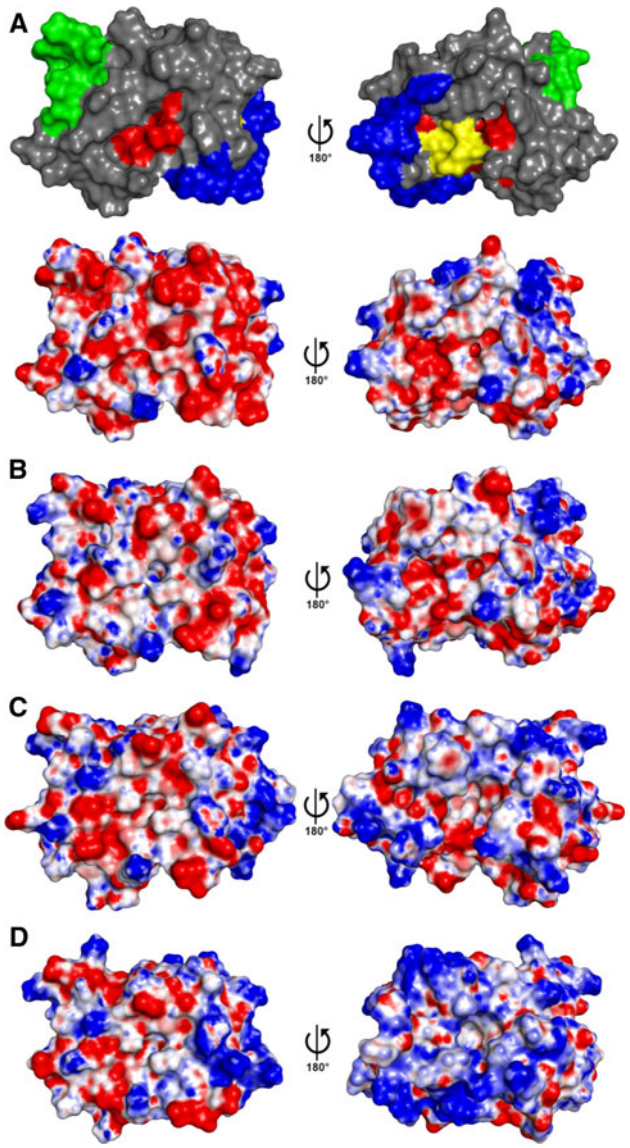

Fig. 6 Comparison of electrostatic surface potentials on functional regions within the three-dimensional structure of snake venom PLA_2 protein family members. **a** $BpirPLA_2$-I (acid Asp49-PLA_2 from *B. pirajai;* this work) **b** BthA-I-PLA_2 (acid Asp49-PLA_2 from *B. jararacussu*), **c** PrTX-III (basic Asp49-PLA_2 from *B. pirajai*), **d** PrTX-I (basic Lys49-PLA_2 from *B. pirajai*). See Table 1 for PDB codes. As a reference, recognized functional regions within the PLA_2 fold are color coded in the top $BpirPLA_2$-I molecular surface in **a**: Active site—*red* (amino acids residues: 48, 49, 52 and 99), Ca^{2+}-binding loop—*yellow* (amino acids residues: 25–34), β-wing—*green* (amino acids residues: 75–77 and 82–84), and C-terminal—*blue* (amino acids residues: 108–133). The remaining molecular surfaces are colored according to the electrostatic potential (<−10 kT/e—*red*, neutral—*white* and >10 kT/e—*blue*). The *left* views facilitate the visualization of the molecular surface facing the active site entrance while views 180°-rotated to the right allow visualization of the Ca^{2+}-binding loop on the opposite face of the molecular surface (color figure online)

In order to gain further insight about the structure–activity relationships among snake venom PLA_2 enzymes, we sought to compare the electrostatic surface potentials on functional regions within the three-dimensional structure of these proteins (Fig. 6). As exposed by the BP analysis above, this was an especially interesting question given the early diversification of positively charged (basic) and negatively charged (acid) PLA_2 enzymes and the importance of functional alterations within the Lys49 clade in *Bothrops* genus. By comparing the top panel in section A of Fig. 6 with either left or right sides of sections B, C, and D, it was possible to map changes in the surface EP of the different snake venom PLA_2 enzymes. In general, most alterations in the EP were observed within the C-terminal region, due to greater variability of charged amino acid residues in this region (Lomonte et al. 2003a, b).

The C-terminal region of cytotoxic Lys49 PLA_2 homologues is characterized by a combination of predominantly cationic and hydrophobic residues. Such composition has been invoked to explain the ability of this region to interact and penetrate phospholipid bilayers, a property that is correlated to the myotoxic activity of these enzymes (Ogawa et al. 1996; Simons and Toomre 2000; Valentin and Lambeau 2000; Lomonte et al. 2003a, b; Ohno et al. 2003; Dos Santos et al. 2009). On the other hand, in $BpirPLA_2$-I, the C-terminal region is predominantly composed by hydrophilic and anionic residues (contains six negatively charged against 3 positively charged residues over 25 residues). Dos Santos et al. (2009) have proposed a myotoxic site in Lys49-PLA_2 enzymes constituted by four residues, three of which are contributed by the C-terminal region (K20, K115, R118, and Y119). The $BpirPLA_2$-I enzyme lacks two of the positively charged residues in the myotoxic site (Lys49-PLA_2: K115, R118, Y119 while in $BpirPLA_2$-I: I115, W118, F119), possibly explaining why this protein does not show myotoxic activity.

Comparison of the EP on the molecular surfaces of the close homologues $BpirPLA_2$-I and BthA-I-PLA_2 (Bjus1 in Fig. 5) revealed that the EP in the active site of $BpirPLA_2$-I is significantly more negative than in BthA-I-PLA_2, even though both enzymes are acid Asp49-PLA_2. On the other hand, the EP on the face opposite to the active site entrance of these molecules (i.e., the region around the calcium binding loop) is well conserved. Interestingly, comparing basic and acid PLA_2 enzymes, the greatest number of changes in the EP from negative to positive occurred in the Ca^{2+} ion binding loop. Such changes on the surface EP in the vicinity of the Ca^{2+} binding site could affect the affinity for the Ca^{2+} ion (by enhancing or reducing the electrostatic stabilization) even if the mutated residues responsible for the change on the surface EP are not directly involved in the Ca^{2+} coordination.

In conclusion, this paper describes the isolation as well as the biochemical, functional, and structural characterization of the first acidic Asp49-PLA_2 (named $BpirPLA_2$-I)

from *Bothrops pirajai* snake venom, and it was demonstrated that a synthetic peptide with a relatively short stretch of amino acids (115–129) near the C-terminal region plays an important role in the antiplatelet activity induced by a svPLA$_2$ showing their potential value as molecular tools or as drug leads in diverse biomedical areas, and the importance of this region for the activity of the hole protein.

Acknowledgments This work was supported by Fundação de Amparo à Pesquisa do Estado de São Paulo (FAPESP), Conselho Nacional de Desenvolvimento Científico e Tecnológico (CNPq) and Instituto Nacional de Ciência e Tecnologia em Toxinas (INCT-Tox), Brazil. We are grateful to Prof. Dr. J. R. Giglio (FMRP-USP) for their manuscript revision; Prof. Dr. A. Nomizo (FCFRP-USP, Brazil), MSc J. Fernández and Prof. Dr. B. Lomonte (ICP, UCR, Costa Rica) for their collaboration in the cytotoxic and hypotension assays. Thank to E. A. Bastos (TT-FAPESP) for their helpful technical collaboration.

References

Andrião-Escarso SH, Soares AM, Rodrigues VM, Angulo Y, Lomonte B, Gutiérrez JM, Giglio JR (2000) Myotoxic phospholipases A_2 in *Bothrops* snake venoms: effects of chemical modifications on the enzymatic and pharmacological properties of Bothropstoxins from *Bothrops jararacussu*. Biochimie 82:755–763

Andrião-Escarso SH, Soares AM, Fontes MRM, Fuly AL, Corrêa FMA, Rosa JC, Greene LJ, Giglio JR (2002) Structural and functional characterization of an acidic platelet aggregation inhibitor and hypotensive Phospholipase A_2 from *Bothrops jararacussu* snake venom. Biochem Pharmacol 64:723–732

Arni RK, Ward RJ (1996) Phospholipase A_2—a structural review. Toxicon 34:827–841

Bowie JU, Luthy R, Eisenberg D (1991) A method to identify protein sequences that fold into a known three-dimensional structure. Science 253:164–169

Cogo JC, Lilla S, Souza GHMF, Hyslop S, De Nucci G (2006) Purification, sequencing and structural analysis of two acidic phospholipases A_2 from the venom of Bothrops insularis (jararaca ilhoa). Biochimie 88:1947–1959

Correa LC, Marchi-Salvador DP, Cintra AC, Sampaio SV, Soares AM, Fontes MR (2008) Crystal structure of a myotoxic Asp49-Phospholipase A_2 with low catalytic activity: insights into Ca^{2+}-independent catalytic mechanism. Biochim Biophys Acta 1784:591–599

Costa TR, Menaldo DL, Oliveira CZ, Santos-Filho NA, Teixeira SS, Nomizo A, Fuly AL, Monteiro MC, de Souza BM, Palma MS, Stábeli RG, Sampaio SV, Soares AM (2008) Myotoxic phospholipases A_2 isolated from *Bothrops brazili* snake venom and synthetic peptides derived from their C-terminal region: cytotoxic effect on microorganism and tumor cells. Peptides 29(10):1645–1656

De Albuquerque Modesto JC, Spencer PJ, Fritzen M, Valença RC, Oliva MLV, da Silva MB, Chudzinski-Tavassi AM, Guarnieri MC (2006) BE-I-PLA$_2$, a novel acidic Phospholipase A_2 from *Bothrops erythromelas* venom: isolation, cloning and characterization as potent anti-platelet and inductor of prostaglandin I_2 release by endothelial cells. Biochem Pharmacol 72:377–384

De Haas GH, Postema NM, Nieuwenhuizen W, van Deenen LLM (1968) Purification and properties of Phospholipase A from porcine pancreas. Biochim Biophys Acta 159:103–117

De Paula R, Castro HC, Rodrigues CR, Melo PA, Fuly AL (2009) Structural and pharmacological features of phospholipases A_2 from snake venoms. Protein Pept Lett 16:899–907

Dos Santos JI, Soares AM, Fontes MRM (2009) Comparative structural studies on Lys49-Phospholipase A_2 from *Bothrops* genus reveal their myotoxic site. J Struct Biol 167:106–116

Edgar RC (2004) MUSCLE: multiple sequence alignment with high accuracy and high throughput. Nucleic Acids Res 32:1792–1797

Fernández J, Gutiérrez JM, Angulo Y, Sanz L, Juárez P, Calvete JJ, Lomonte B (2010) Isolation of an acidic phospholipase A_2 from the venom of the snake *Bothrops asper* of Costa Rica: biochemical and toxicological characterization. Biochimie 92:273–283

Fuly AL, de Miranda AL, Zingali RB, Guimarães JA (2002) Purification and characterization of a phospholipase A_2 isoenzyme isolated from *Lachesis muta* snake venom. Biochem Pharmacol 63:1589–1597

Gebrim LC, Marcussi S, Menaldo DL, de Menezes CS, Nomizo A, Hamaguchi A, Silveira-Lacerda EP, Homsi-Brandeburgo MI, Sampaio SV, Soares AM, Rodrigues VM (2009) Antitumor effects of snake venom chemically modified Lys49 phospholipase A_2-like BthTX-I and a synthetic peptide derived from its C-terminal region. Biologicals 37(4):222–229

Gonnet GH, Cohen MA, Benner SA (1992) Exhaustive matching of the entire protein sequence database. Science 256:1443–1445

Guda C, Scheeff ED, Bourne PE, Shindyalov IN (2001) A new algorithm for the alignment of multiple protein structures using Monte Carlo optimization. Pac Symp Biocomput 6:275–286

Gutiérrez JM, Lomonte B (1997) In: Kini RM (ed) Venom Phospholipase A_2 enzymes: structure, function and mechanism. Wiley, Chichester, pp 321–352

Gutiérrez JM, Avila C, Rojas E, Cerdas L (1988) An alternative in vitro method for testing the potency of the polyvalent antivenom produced in Costa Rica. Toxicon 26:411–413

Hall TA (1999) BioEdit: a user-friendly biological sequence alignment editor and analysis program for Windows 95/98/NT. Nucl Acids Symp Ser 41:95–98

Harris JB, Grubb BD, Maltin CA, Dixon R (2000) The neurotoxicity of the venom Phospholipases A_2; notexin and taipoxin. Exp Neurol 161:517–526

Huang HC, Lee CY (1984) Isolation and pharmacological properties of phospholipases A_2, from *Vipera russelli* (Russell's viper) snake venom. Toxicon 22:207–217

Jones DT, Taylor WR, Thornton JM (1992) The rapid generation of mutation data matrices from protein sequences. Comp Appl Biosci 8:275–282

Ketelhut DFJ, Homem de Mello M, Veronese ELG, Esmeraldino LE, Murakami MT, Arni RK, Giglio JR, Cintra ACO, Sampaio SV (2003) Isolation, characterization and biological activity of acidic phospholipase A_2 isoforms from *Bothrops jararacussu* snake venom. Biochimie 85:983–991

Korkmaz B, Attucci S, Juliano MA, Kalupov T, Jourdan ML, Juliano L, Gauthier F (2008) Measuring elastase, proteinase 3 and cathepsin G activities at the surface of human neutrophils with fluorescence resonance energy transfer substrates. Nat Protoc 3:991–1000

Laemmli UK (1970) Cleavage of structural proteins during the assembly of the head of bacteriophage T4. Nature 227:680–685

Laskowski RA, MacArthur MW, Moss DS, Thornton JM (1993) PROCHECK: a program to check the stereochemical quality of protein structures. J Appl Cryst 26:283–291

Lomonte B, Angulo Y, Calderón L (2003a) An overview of lysine-49 phospholipase A_2 myotoxins from crotalid snake venoms and their structural determinants of myotoxic action. Toxicon 42:885–901

Lomonte B, Angulo Y, Santamaría C (2003b) Comparative study of synthetic peptides corresponding to region 115–129 in Lys49

myotoxic phospholipases A_2 from snake venoms. Toxicon 42:307–312

Lomonte B, Angulo Y, Moreno E (2010) Synthetic peptides derived from the C-terminal region of Lys49 phospholipase A2 homologues from viperidae snake venoms: biomimetic activities and potential applications. Curr Pharm 16(28):3224–3230

Lu QM, Jin Y, Wei JF, Wang WY, Xiong YL (2002) Biochemical and biological properties of *Trimeresurus jerdonii* venom and characterization of a platelet aggregation-inhibiting acidic phospholipase A_2. J Nat Toxins 11:25–33

Luthy R, Bowie JU, Eisenberg D (1992) Assessment of protein models with three-dimensional profiles. Nature 356:83–85

MacKerell AD Jr, Brooks B, Brooks CL III, Nilsson L, Roux B, Won Y, Karplus M (1998) CHARMM: the energy function and its paramerization with an overview of the program. In: Schleyer PVR, Allinger NL, Clark T, Gasteiger J, Kollman PA, Schaefer HF III, Schreiner PR (eds) Encyclopedia of computational chemistry. Wiley, Chichester, pp 271–277

Magro AJ, Takeda AAS, Soares AM, Fontes MRM (2005) Structure of BthA-I complexed with p-bromophenacyl bromide: possible correlations with lack of pharmacological activity. Acta Crystallogr D 61:1670–1677

Marchi-Salvador DP, Fernandes CAH, Amui SF, Soares AM, Fontes MRM (2006) Crystallization and preliminary X-ray diffraction analysis of a myotoxic Lys49-PLA_2 from *Bothrops jararacussu* venom complexed with *p*-bromophenacyl bromide. Acta Crystallogr 62F:600–603

Marchi-Salvador DP, Correa LC, Magro AJ, Oliveira CZ, Soares AM, Fontes MR (2008) Insights into the role of oligomeric state on the biological activities of crotoxin: crystal structure of a tetrameric phospholipase A_2 formed by two isoforms of crotoxin B from *Crotalus durissus terrificus* venom. Proteins 72:883–891

Marchi-Salvador DP, Fernandes CA, Silveira LB, Soares AM, Fontes MR (2009) Crystal structure of a phospholipase A_2 homologue complexed with p-bromophenacyl bromide reveals important structural changes associated with the inhibition of myotoxic activity. Biochim Biophys Acta 1794:1583–1590

Murakami MT, Gabdoulkhakov A, Genov N, Cintra AC, Betzel C, Arni RK (2006) Insights into metal ion binding in phospholipases A_2: ultra high-resolution crystal structures of an acidic phospholipase A_2 in the Ca^{2+} free and bound states. Biochimie 88:543–549

Murillo LA, Lan CY, Agabian NM, Larios S, Lomonte B (2007) Fungicidal activity of a phospholipase-A2-derived synthetic peptide variant against *Candida albicans*. Rev Esp Quimioter 20(3):330–333

Notredame C, Higgins DG, Heringa J (2000) T-Coffee: a novel method for fast and accurate multiple sequence alignment. J Mol Biol 302:205–217

Ogawa T, Nakashima K-I, Nobuhisa I, Deshimaru M, Shimohigashi Y, Fukumak Y, Sakaki Y, Hattori S, Ohno M (1996) Accelerated evolution of snake venom phospholipase a, isozymes for acquisition of diverse physiological functions. Toxicon 34:1229–1236

Ohno M, Chijiwa T, Oda-Ueda N, Ogawa T, Hattori S (2003) Molecular evolution of myotoxic phospholipases A_2 from snake venom. Toxicon 42:841–854

Ownby CL, Selistre-de-Araujo HS, White SP, Flecther JE (1999) Lysine 49 phospholipase A_2 proteins. Toxicon 37:411–445

Renetseder R, Brunie S, Dijkstra BW, Drenth J, Sigler PB (1985) A comparison of the crystal structures of phospholipases A_2 from bovine pancreas and *Crotalus atrox* venom. J Biol Chem 260:11627–11636

Roberto PG, Kashima S, Soares AM, Chioato L, Faça VM, Fuly AL, Astolfi-Filho S, Pereira JO, França SC (2004) Cloning and expression of an acidic platelet aggregation inhibitor phospholipase A_2 cDNA from *Bothrops jararacussu* venom gland. Protein Expr Purif 37:102–108

Rocchia W, Alexov E, Honig B (2001) Extending the applicability of the nonlinear poisson-boltzmann equation: multiple dielectric constants and multivalent ions. J Phys Chem 105B:6507–6514

Rodrigues RS, Izidoro LF, Teixeira SS, Silveira LB, Hamaguchi A, Homsi-Brandeburgo MI, Selistre-de-Araujo HS, Giglio JR, Fuly AL, Soares AM, Rodrigues VM (2007) Isolation and functional characterization of a new myotoxic acidic phospholipase A_2 from *Bothrops pauloensis* snake venom. Toxicon 50:153–165

Ronquist F, Huelsenbeck JP (2003) MRBAYES 3: Bayesian phylogenetic inference under mixed models. Bioinformatics 19:1572–1574

Sali A, Blundell TL (1993) Comparative protein modelling by satisfaction of spatial restraints. J Mol Biol 234:779–815

Santos-Filho NA, Silveira LB, Oliveira CZ, Bernardes CP, Menaldo DL, Fuly AL, Arantes EC, Sampaio SV, Mamede CCN, Beletti ME, Oliveira F, Soares AM (2008) A new acidic myotoxic, antiplatelet and prostaglandin I_2 inductor phospholipase A_2 isolated from *Bothrops moojeni* snake venom. Toxicon 52:908–917

Schaloske RH, Dennis EA (2006) The Phospholipase A_2 superfamily and its group numbering system. Biochim Biophys Acta 1761:1246–1259

Serrano SMT, Reichl AP, Mentele R, Auerswld EA, Santoro ML, Sampaio CAM, Camargo ACM, Assakura MT (1999) A novel Phospholipase A_2, Bj-PLA_2, from the venom of the snake *Bothrops jararaca*: purification, primary structure analysis, and its characterization as a platelet-aggregation-inhibiting factor. Arch Biochem Biophys 367:26–32

Shen MY, Sali A (2006) Statistical potential for assessment and prediction of protein structures. Protein Sci 15:2507–2524

Simons K, Toomre D (2000) Lipid rafts and signal transduction. Nat Rev Mol Cell Biol 1:31–39

Sitkoff D, Sharp KA, Honig B (1994a) Accurate calculation of hydration free energies using macroscopic solvent models. J Phys Chem 98:1978–1988

Sitkoff D, Lockhart DJ, Sharp KA, Honig B (1994b) Calculation of electrostatic effects at the amino terminus of an alpha helix. Biophys J 67:2251–2260

Soares AM, Giglio JR (2003) Chemical modifications of phospholipases A_2 from snake venoms: effects on catalytic and pharmacological properties. Toxicon 42:855–868

Soares AM, Fontes MRM, Giglio JR (2004) Phospholipase A_2 myotoxins from *Bothrops* snake venoms: structure-function relationship. Curr Org Chem 8:1–14

Valentin E, Lambeau G (2000) What can venom phospholipases A_2 tell us about the functional diversity of mammalian secreted phospholipases A_2? Biochimie 82:815–831

Vesterberg O (1972) Isoelectric focusing of proteins in polyacrylamide gels. Biochim Biophys Acta 257:11–13

Whelan S, Goldman N (2001) A general empirical model of protein evolution derived from multiple protein families using a maximum-likelihood approach. Mol Biol Evol 18:691–699

Zuccon A, Zuccon D (2008) Program distributed by the authors. http://www.mrent.org